

The Cause of the Superoutburst in SU UMa Stars is Finally Revealed by Kepler Light Curve of V1504 Cygni

Yoji OSAKI

Department of Astronomy, School of Science, University of Tokyo, Hongo, Tokyo 113-0033
osaki@ruby.ocn.ne.jp

and

Taichi KATO

Department of Astronomy, Kyoto University, Sakyo-ku, Kyoto 606-8502
tkato@kusastro.kyoto-u.ac.jp

(Received 2012 November 19; accepted 2012 December 7)

Abstract

We have studied the short cadence Kepler light curve of an SU UMa star, V1504 Cyg, which covers a period of ~ 630 d. All superoutbursts in V1504 Cyg have turned out to be of precursor-main types, and the superhump first appears near the maximum of the precursor. The superhumps grow smoothly from the precursor to the main superoutburst, showing that the superoutburst was initiated by a tidal instability (as evidenced by the growing superhump) as envisioned in the thermal-tidal instability (TTI) model proposed by Osaki (1989, PASJ, 41, 1005). We performed a power spectral analysis of the light curve of V1504 Cyg. One of the outstanding features is the appearance of a negative superhump extending over around 300 d, well over a supercycle. We found that the appearance of the negative superhump tends to decrease the frequency of occurrence of normal outbursts. Two types of supercycles are recognized in V1504 Cyg, which are similar to those of the Type L and Type S supercycles in the light curve of VW Hyi, a prototype SU UMa star, introduced by Smak (1985, Acta Astron., 35, 357). It is found that the Type L supercycle is the one accompanied by the negative superhump, and Type S is that without the negative superhump. If we adopt a tilted disk as an origin of the negative superhump, two types of the supercycles are understood to be due to a difference in the outburst interval, which is in turn caused by a difference in mass supply from the secondary to different parts of the disk. The frequency of the negative superhump varies systematically during a supercycle in V1504 Cyg. This variation can be used as an indicator of the disk-radius variation, and we have found that the observed disk-radius variation in V1504 Cyg fits very well with a prediction of the TTI model.

Key words: accretion, accretion disks — stars: dwarf novae — stars: individual (V1504 Cygni) — stars: novae, cataclysmic variables

1. Introduction

The SU UMa stars are dwarf novae in short orbital periods that show two distinct types of outbursts: a short normal outburst with a duration of a few days, and a long superoutburst with a duration of typically two weeks [see, Warner (1995) and Hellier (2001a) for dwarf novae in general and for SU UMa stars in particular]. In ordinary SU UMa stars, several short normal outbursts are sandwiched between two long superoutbursts, and a cycle from one superoutburst to the next is called a supercycle. Normal outbursts are believed to be essentially the same as those outbursts observed in ordinary dwarf novae with a longer orbital period, such as U Gem and SS Cyg stars; they are now well understood by considering the thermal limit-cycle instability in the accretion disk (see, e.g., Cannizzo 1993; Lasota 2001). During the superoutburst, periodic humps, called the superhumps, always appear with a period slightly longer than the orbital period by a few percent. The superhump phenomenon is now well understood by considering the tidal instability

(Whitehurst 1988; Hirose, Osaki 1990; Lubow 1991); superhumps are produced by a periodic tidal stressing of the eccentric precessing accretion disk, which is in turn produced by the tidal 3:1 resonance instability between the accretion-disk flow and the orbiting secondary star.

As to the superoutburst and supercycle of SU UMa stars, three different models have so far been proposed: the thermal-tidal instability model advocated by Osaki, the enhanced mass-transfer model advocated by Smak, and the pure thermal instability model by Cannizzo. No consensus has yet been reached about the cause of the superoutburst.

Besides the original planet hunting mission, NASA's Kepler observations (Koch et al. 2010) with high-accuracy photometry give an unprecedented opportunity to investigate variable stars. Two SU UMa stars, V344 Lyr and V1504 Cyg, in the Kepler field have been observed with the short cadence (SC) mode, and some of their light curves are now available to the public. In this paper, we consider the cause of the superoutburst in SU UMa stars using the Kepler light curve of one of them, V1504 Cyg,

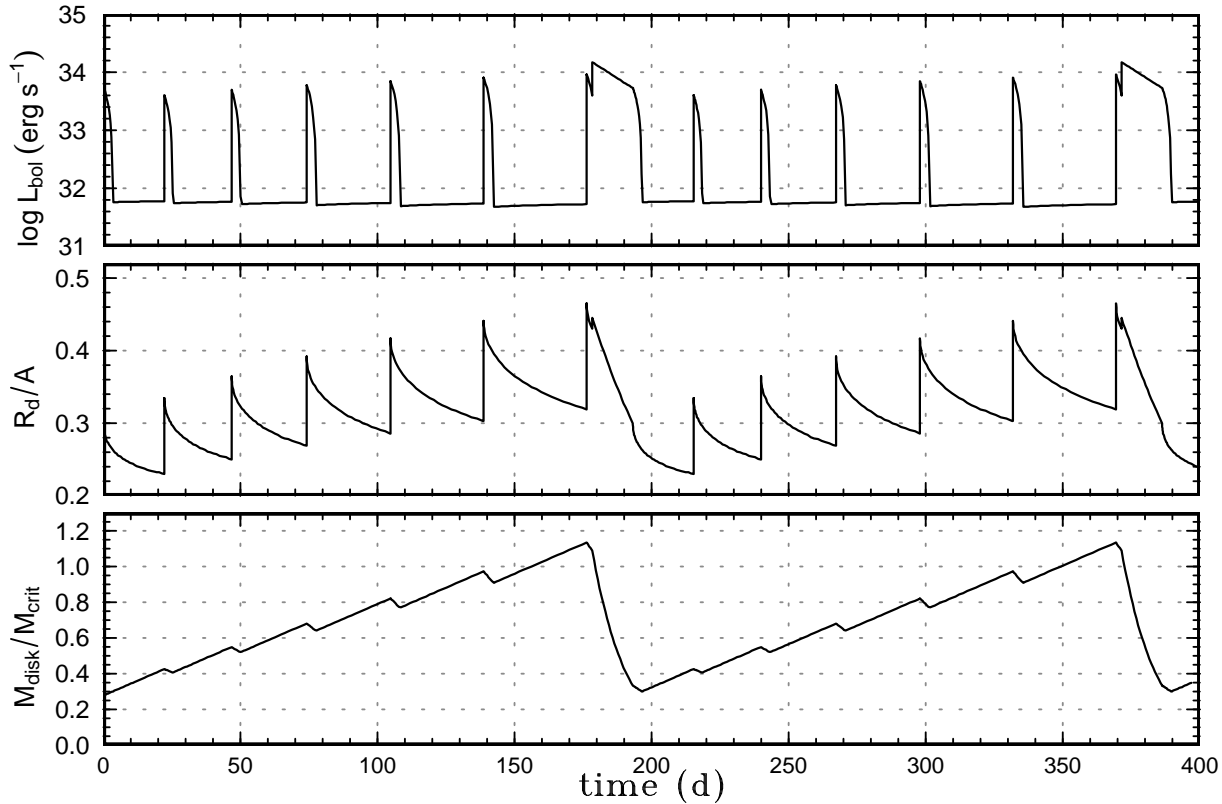


Fig. 1. Time evolution of an accretion disk in a supercycle based on the simplified form of the TTI model, redrawn by using the result in Osaki (2005). Two supercycles are shown in the figure for clarity. The model parameters used are those of VW Hya, a prototype SU UMa star. From the top to the bottom: bolometric light curve, the disk-radius variation in units of the binary separation A , the total disk mass, M_{disk} , normalized by the critical mass M_{crit} above which the disk can be tidally unstable.

in section 3.

Before going into our study of Kepler data, we first review three models for superoutbursts and supercycles of SU UMa stars in section 2. For convenience, we summarize in table 1 main differences among the three models and what we regard as being consequences of these models to be compared with observations.

2. Superoutburst Models

2.1. Thermal-tidal Instability Model (TTI Model)

About the superoutburst and supercycle of SU UMa stars, Osaki (1989) proposed a model (now called the thermal-tidal instability model, or TTI model in short) in which the ordinary thermal instability is coupled with the tidal instability [see, Osaki (1996) for a review]. The TTI model is basically of the disk-instability variety, in which the mass-transfer rate from the secondary is assumed to be constant, and all variability is thought to be produced within the disk.

The TTI model explains the supercycle of SU UMa stars in the following way. In the initial stage of the supercycle, the disk is assumed to be compact well below the 3:1 resonance radius. A successive outburst (normal outburst) causes mass accretion onto the central white dwarf, but the accreted mass is less than the mass transferred in quiescence. The mass and the angular momentum of the

disk accumulate and the disk's outer edge therefore grows with a succession of normal outbursts, and the final normal outburst (a triggering normal outburst) brings disk's outer edge beyond the 3:1 resonance radius $R_{3:1}$ (where $R_{3:1} \simeq 0.46A$ and A is the binary separation). The disk then becomes tidally unstable, and a circular disk is transformed to a slowly precessing eccentric disk. The tidal dissipation of the eccentric disk now enhances the mass flow in the disk, sustaining a hot state of the disk so as to cause a longer superoutburst. When sufficient mass is drained from the disk, the surface density of matter in the outer edge reaches the critical one, below which no hot state exists. The disk makes a downward transition to a cool state. The cooling front propagates inward, extinguishing the outburst, i.e., an end of the superoutburst. The eccentric disk eventually returns to a circular one because of the addition of matter of low specific angular momentum. Because of the enhanced tidal torque during the superoutburst stage, the disk becomes compact in the end. A new supercycle begins. This is the basic picture of the TTI model, but a minor modification and a further refinement of this model have been proposed by Hellier (2001b), Osaki, Meyer (2003), Osaki (2005).

Osaki (1989) has calculated light curves of SU UMa stars by using a simplified semianalytic model, consisting of a torus and an inviscid disk having a power-law

Table 1. Comparison of models for superoutbursts and superhumps.

Models			
	thermal-tidal instability (TTI)	enhanced mass-transfer (EMT)	pure thermal instability
major advocator	Osaki	Smak	Cannizzo
mass-transfer rate from the secondary (\dot{M}_{tr})	constant	variable	constant
origin of superhump	eccentric disk	variable hot spot brightness	(eccentric disk?)
origin of superoutburst	enhanced tidal torque	enhanced mass-transfer	wide outburst
main point of the model	disk radius variation in supercycle	EMT due to irradiation of the secondary	pure thermal instability is complex enough to produce superoutburst and supercycle
major premises of the model	(1) constant \dot{M}_{tr} (2) tidal instability and eccentric disk responsible for superhump and superoutburst	(1) enhanced mass transfer from the secondary due to irradiation heating (2) variable and enhanced hot spot during superoutburst	(1) pure thermal instability (2) superhump is of secondary importance (3) normal outbursts are “inside-out”
Major consequences discussed in this paper [†]			
expansion of the disk during normal outburst	Yes	Yes	<u>No</u>
outside-in type normal outburst	Yes	NA*	<u>No</u>
humps during the last normal outburst before superoutburst	failed superhumps	<u>enhanced hot spot</u>	NA
distinct precursor outburst	Yes	Yes	<u>No</u>
appearance of superhump	peak of precursor	<u>after peak of superoutburst</u>	NA
enhanced hot spot during superoutburst	No	<u>Yes</u>	No

[†]Underlined items are not in agreement with observation or items need to be explained by the model (see text for details).

*Not applicable.

surface-density distribution. Figure 1 illustrates one of such light curves together with the disk-radius variation and the disk-mass variation. Here, we note that all outbursts in this model are of “outside-in” (here “outside-in” means an outburst in which a transition to the hot state first occurs at the outer part of the disk and the heating wave propagates inward, while “inside-out” does that in which a transition to the hot state occurs at its inner part and the heating wave propagates outward).

As far as the mass accumulated during a supercycle is concerned, the difference between a normal outburst just prior to a superoutburst and the next superoutburst is rather small, as can be seen in the lowest panel of figure 1. However, there is a big difference between these two states concerning the tidal removal of angular momentum from the disk. In the case of a normal outburst, the disk’s outer edge is below the tidal 3:1 resonance radius, and thus the tidal removal of angular momentum is very ineffective. On the other hand, the disk’s outer edge exceeds the tidal 3:1 resonance radius in the last normal outburst or the triggering outburst (which is a part of precursor of a superoutburst). The tidal instability then develops, which is observationally seen as growing superhumps. As discussed in Osaki, Meyer (2003) and Osaki (2005), in the case of no effective tidal removal of angular momentum from the disk, an expansion of the disk due to the thermal instability immediately returns the surface density at the outer edge of the disk to the critical density below which there exists no hot state. The disk then makes a downward transition to the cool state and the cooling wave propagates inward and the outburst is short. This is the reason why the normal outburst just prior to a superoutburst is so short, even if mass is sufficiently accumulated in the disk.

The key point of the TTI model lies in the disk-radius variation shown in the middle panel of figure 1. This must be tested observationally but it had been difficult before the Kepler observations

Ichikawa et al. (1993) have performed light-curve simulations of the superoutburst and supercycle of SU UMa stars by using a one-dimensional numerical code based on the TTI model. Two different prescriptions for the viscosity in the cold state (i.e., α_{cold}) have been examined there. One is a case of outside-in normal outbursts where the α viscosity has a radial dependence (called there “case A”); the other is an inside-out case (“case B”) where the α viscosity is constant with respect to the radius. It has been shown that quiescent intervals between normal outbursts increase monotonously with the advance of supercycle phase in case A (see, their figure 1) while they stay almost constant during the supercycle in case B (see, their figure 2). This point will be discussed later together with Kepler light curves. Buat-Ménard, Hameury (2002) have performed light curve simulations by using their code, confirming that the TTI model can account for SU UMa light curves. Two-dimensional smoothed particle hydrodynamics (SPH) code simulations of superhumps and superoutbursts of SU UMa stars were performed by Murray (1998) and Truss et al. (2001), confirming that the superoutburst

and superhump phenomena are a direct result of the tidal instability. Smith et al. (2007) made 3D SPH simulations of superhumps, and found such enhanced tidal torques as to transfer the angular momentum from the disk to the binary’s orbital motion when the eccentric instability develops, as suggested in the TTI model.

Two alternative models to explain the superoutburst phenomenon have been proposed besides the TTI model. One is the enhanced mass-transfer model (EMT model) due to irradiation heating of the secondary star, advocated by Smak. The other is the pure thermal instability model by Cannizzo et al. (2010).

2.2. The Enhanced Mass-Transfer Model (EMT Model)

The enhanced mass-transfer model for superoutbursts of SU UMa stars was first proposed by Vogt (1983), and discussed by Osaki (1985). In this model, the superoutburst of SU UMa stars is produced by enhanced mass transfer from the secondary star, which is in turn caused by irradiation heating of the secondary star. Osaki (1985) proposed an EMT model, a model of the irradiation-induced mass-overflow instability as a possible cause of superoutbursts in SU UMa stars. However, Osaki (1996) abandoned this model later in favor of the TTI model. Smak pursued this model instead.

Smak (1991), Smak (2004), Smak (2008) has been writing a series of papers in *Acta Astronomica* in which he criticizes the TTI model, and instead he advocates the enhanced mass-transfer (EMT) model. In the EMT model, the long duration of the superoutburst of SU UMa stars is thought to be produced by the enhanced mass transfer from the secondary star, which is in turn caused by irradiation heating of the atmosphere of the secondary star due to ultraviolet radiation from the mass-accreting white dwarf and the boundary layer between the accretion disk and the central white dwarf. In the EMT model the superhump phenomenon is not directly related to the mechanism of the superoutburst. Rather, the superhump is thought to be produced by a modulated dissipation of the gas stream due to modulated mass outflow, which is in turn produced by periodically variable irradiation of the secondary star (Smak 2009).

As Smak (1991), Smak (1996), Smak (2000) clearly stated, he was motivated to pursue the EMT model because of following two seeming difficulties in the TTI model, to which we address ourselves in this paper:

1. Observational evidence for enhanced mass transfer: Vogt (1983) argued in his review of VW Hyi that the amplitude of its orbital humps increases in maximum or declining stage of normal outbursts if they occur less than 40 d before the next following superoutburst, and interpreted that the mass-transfer rate from the secondary star is enhanced. Smak (1991) regarded this point as one of the difficulties of the TTI model.
2. Sequence of events that the TTI model predicts: Smak raised another question concerning the TTI model, which is connected with the sequence of

events responsible for superoutbursts and superhumps. He argued that in the TTI model the sequence begins with a tidal instability, leading to the formation of an eccentric disk, and causing a major enhancement of the accretion rate. Accordingly, the superhump should appear at the very early phase of a superoutburst (certainly not later than maximum). In most cases, however, it appears one or two days *after the superoutburst maximum*.

As regards point 1, Osaki, Meyer (2003) already questioned Vogt’s interpretation of “orbital humps”, and suspected that observed humps could be of a superhump nature. This is the very controversy about the nature of observed humps. These two problems raised by Smak will be discussed while considering the Kepler light curve of V1504 Cyg.

Light-curve simulations based on the EMT model were made by Smak (1991) and Schreiber et al. (2004). Schreiber et al. (2004) performed light-curve simulations in both the TTI model and the EMT model, and they compared their results with multiwavelength light curves of VW Hyi, one of the best observed SU UMa stars before the Kepler observations. All outbursts in their models turned out to be of the inside-out type because of their viscosity prescription. It was found there that both models can generate precursor outbursts that are more pronounced at shorter wavelengths, which is in agreement with observations. Since there are adjustable free-parameters in the numerical light-curve simulations for both the TTI model and the EMT model, Schreiber et al. (2004) stated that it is difficult to decide which model is better for explaining observations. However, these authors have concluded that the EMT model should be favored over the TTI model because the EMT model is more sensitive to any mass-transfer rate variation, which is supposed by these authors to be responsible for variations seen in different supercycles in one star and in different SU UMa stars.

In the EMT model, the mass-transfer rate is thought to be greatly increased during a superoutburst. The response of the secondary’s envelope to enhanced mass transfer has to be considered. That is, the response of the mass reservoir of the envelope of the secondary will affect the recurrence time of the supercycle in SU UMa stars. This effect has not been taken into account in the simulations of Schreiber et al. (2004), and their results are thus incomplete in this respect.

2.3. The Pure Thermal Limit Cycle Model

Let us now turn to another alternative, the pure thermal instability model proposed by Cannizzo et al. (2010), Cannizzo et al. (2012) and references therein. In this model, the short normal outburst and the long superoutburst of SU UMa stars are thought to be “narrow” and “wide” outbursts seen in SS Cyg-type dwarf novae of longer orbital period systems, respectively. This is an idea first proposed by van Paradijs (1983). In this model, not only the short normal outburst, but also the long su-

peroutburst is explained by the standard thermal limit cycle instability, and the tidal instability is not needed to explain the long duration of the superoutburst and the supercycle phenomenon in SU UMa stars. The superhump is only an additional phenomenon, and it is of secondary importance. Cannizzo et al. (2010) performed numerical simulations, demonstrating that the thermal limit cycle instability without any tidal instability is complex enough to produce the superoutburst and the supercycle of SU UMa stars in which several short outbursts are sandwiched by two long outbursts.

In Cannizzo’s pure thermal limit-cycle model, the short normal outburst is explained by an inside-out outburst in which an outburst is started in the inner part of the accretion disk and the heating front propagates outward, but it does not reach the disk’s outer edge and is reflected in the middle of the disk as a cooling wave [see, figures 3 and 4 of Cannizzo et al. (2010)]. This type of outburst is called as “Type Bb” in Smak’s classification, and it is known that the disk’s outer edge does not expand in this type of outburst, even when an outburst occurs (see Smak 1984). In this model, the mass in the outer part of the disk is untapped during short normal outbursts, but only the mass in the inner part is accreted during these outbursts. The triggering outburst in this model is also the inside-out outburst, but this time the heating front traveling outward finally reaches the disk’s outer edge, producing a long superoutburst with the viscous plateau stage (i.e., Smak’s Type Ba outburst).

As discussed by Smak (1984), an alternation of narrow and wide outbursts can be produced in the case of the inside-out outbursts. On the other hand, in the case of the outside-in outbursts, the widths of outbursts are more or less similar. If any normal outburst in SU UMa stars turns out to be outside-in based on observations, Cannizzo’s model will meet a serious difficulty. We discuss below Cannizzo’s pure thermal instability model as well.

3. Kepler Light Curve of V1504 Cyg

Kepler observations now open a possibility of discriminating between these three models of SU UMa stars from a purely observational point of view. Two SU UMa-type dwarf novae, V1504 Cyg and V344 Lyr, were observed with the short cadence mode by the Kepler satellite. These light curves have already been studied by Cannizzo and his group, i.e., concerning quiescent superhumps (Still et al. 2010), numerical models of the long term light curve of V344 Lyr (Cannizzo et al. 2010), studies of both positive and negative superhumps in the long term light curve of V344 Lyr (Wood et al. 2011), and a study of the outburst properties of V1504 Cyg and V344 Lyr (Cannizzo et al. 2012). In this paper we examine the same Kepler data of V1504 Cyg, but from a different point of view. Data that we have used in this paper extend over the period from 2009 June to 2011 March. We discuss three problems: the global light curve (subsection 3.1), the way superoutbursts start (subsection 3.2), and the negative superhump (subsections 3.3 and 3.4). As shown

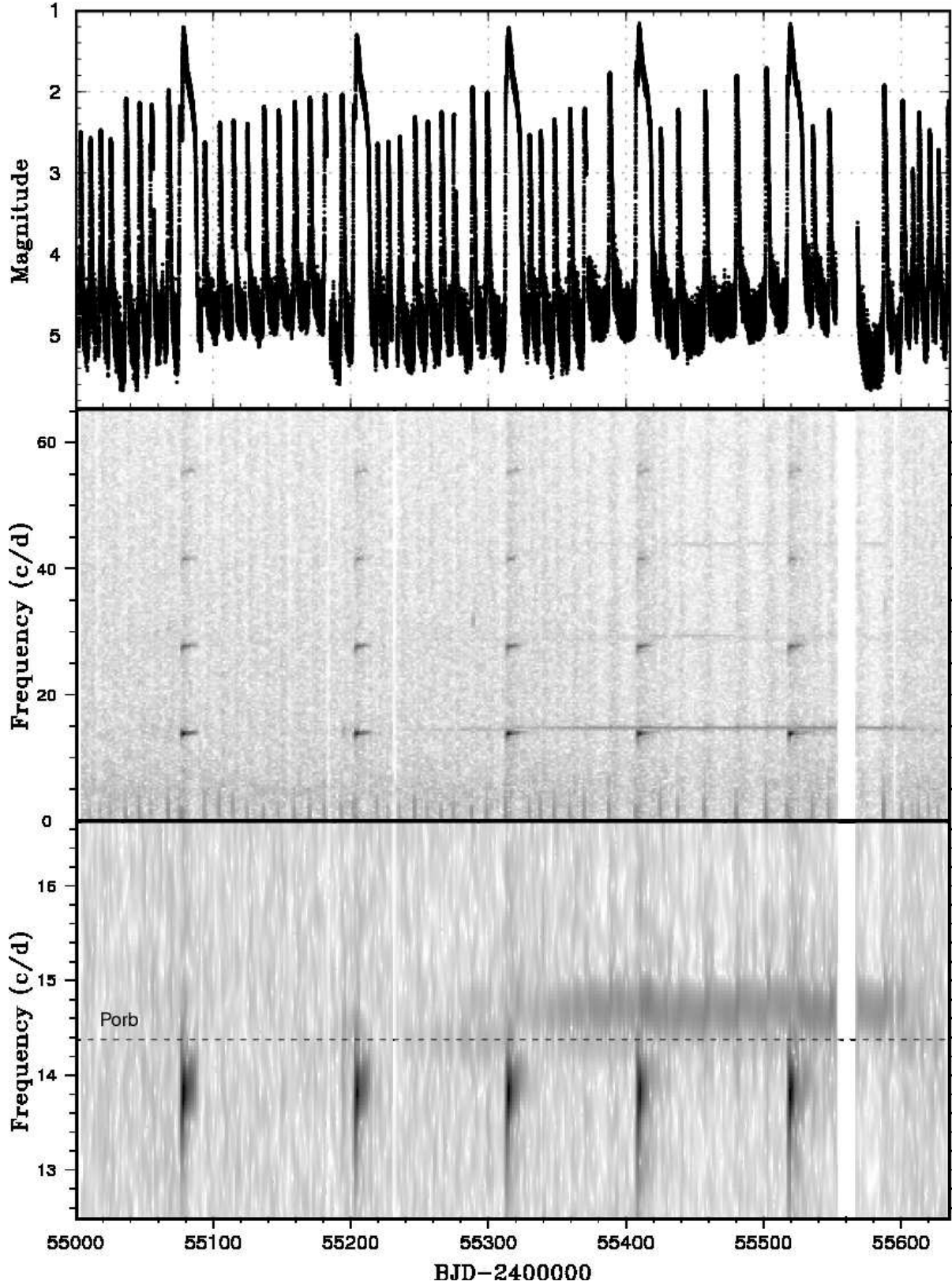


Fig. 2. Two-dimensional power spectrum of the Kepler light curve of V1504 Cyg for the all data. From the top to the bottom, (upper:) light curve; the Kepler data were binned to 0.005 d, (middle:) power spectrum, (lower:) its enlargement for the frequency region around the orbital one. The width of the moving window and the time step used are 5 d and 0.5 d, respectively.

Table 2. Superoutbursts and supercycles of V1504 Cyg.*

(1) SC number	(2) start of SC [†]	(3) start of SO [†]	(4) end of SO [†]	(5) SC length excluding SO [‡]	(6) SO duration [‡]	(7) SC length [‡]	(8) number of NO	(9) negative SH	(10) orbital hump
1	–	74.5	88.5	–	14	>88	>8	no	no
2	88.5	201	215	112.5	14	126.5	10	no	no
3	215	312	325	97	13	110	10	later half	partly
4	325	406.5	419	81.5	12.5	94	6	full	no
5	419	516	530	97	14	111	5	full	no
6	530	–	–	–	–	–	–	early part	later part

*Abbreviations in this table: supercycle (SC), superoutburst (SO), normal outburst (NO), superhump (SH).

[†]BJD–2455000.

[‡]Unit: d.

below, we have reached quite a different conclusion from that of Cannizzo et al. (2012) concerning the nature of the superoutburst and supercycle.

3.1. Global Light Curves and Supercycles of V1504 Cyg

The Kepler light curves of V1504 Cyg and V344 Lyr, extending over 736 d at 1 min cadence, have been examined by Cannizzo et al. (2012); they have studied various correlations, such as quiescence intervals between normal outbursts for the period of one supercycle. Here, we examine the same data set of V1504 Cyg from a different standpoint. The data we used are those of a public release of 632 d at 1 min cadence. Since Wood et al. (2011) examined V344 Lyr, we examine data of V1504 Cyg here.

The Kepler light curve of V1504 Cyg was already studied by Kato et al. (2012). We summarize the basic data of V1504 Cyg obtained there; its orbital period is 0.069549 d (1.67 hr or 14.38 c/d), the (ordinary or positive) superhump period ~ 0.072 d (13.8 c/d), and the negative superhump period ~ 0.068 d (14.7 c/d).

We made a two-dimensional power spectral analysis (the dynamic spectrum) of the light curve of V1504 Cyg, and show our results together with the light curve in figure 2. We used the Kepler raw data (SAP_FLUX) during the period of 632 d from Barycentric Julian Date (BJD) 2455002 to 2455635. In calculating the power spectra, we used a locally-weighted polynomial regression (LOWESS: Cleveland 1979) to Kepler magnitudes (on an arbitrary zero-point) for removing trends resulting from outbursts using smoothing parameters ($f=0.0003$, $\delta=0.2$) in R software¹. We then estimated the pulsed flux by multiplying the residual amplitudes and LOWESS-smoothed light curve converted to the flux scale. In calculating the Fourier spectrum, we used a Hann window function with a 5 d width of the moving window, and 0.5 d as the time step. Figure 2 shows the overall light curve in the top panel, power spectra in a wider frequency range in the middle, and their enlarged portion near the orbital frequency of the star in the bottom, since we are interested in this region.

Let us first look at figure 2 for light curve of V1504 Cyg. The Kepler data of V1504 Cyg we use here include five superoutbursts and four supercycles; we summarize their main characteristics in table 2. Here, we define the start of a supercycle as "the start of quiescence just after the preceding superoutburst" and its end as "the end of the superoutburst." The first column (1) of table 2 is the supercycle ordinal number of our data, while the next three columns give (2) BJD of the start of a supercycle, (3) the start of a superoutburst, and (4) BJD of the end of the superoutburst counted from BJD 2455000. Thus the date of the start of a supercycle is the same as that of the end of the preceding superoutburst, as can be seen in the table. The following three columns give the lengths in days of a supercycle excluding superoutburst (5), of the superoutburst duration (6), and of the full supercycle (7), respectively; thus the sum of the two columns, (5) and (6), is equal to column (7). The next column (8) gives number of normal outbursts during a supercycle. The last two columns, (9) and (10), give comments on the appearance (or visibility) of negative superhumps and orbital humps in the power spectrum of figure 2, respectively, where "no" means no strong signals in the power spectrum. We have four complete supercycles No. 2–5, while supercycles No. 1 and No. 6 are incomplete because they are lacking in the preceding and the following superoutbursts, respectively.

As can be seen in the light curve of figure 2 and in table 2, one of the most outstanding features in supercycles of V1504 Cyg is that the number of normal outbursts during a supercycle differs greatly from supercycle to supercycle, i.e., it varies from 5 (for supercycle No. 5) to 10 (for supercycles No. 2 and No. 3) in the case of V1504 Cyg. Although the duration of the supercycle differs among different supercycles (its average value is ~ 110 d in V1504 Cyg), its difference is small as compared with the difference in the number of outbursts among different supercycles. The duration of superoutbursts does not differ much in different supercycles, either. This point will be discussed later in this subsection.

Let us now examine the power spectra shown in the middle and lower panels of figure 2, and also those of individual supercycles in figure 3 for more details where a frequency 14.38 c/d for the orbital period is indicated by

¹ The R Foundation for Statistical Computing:
<<http://cran.r-project.org/>>.

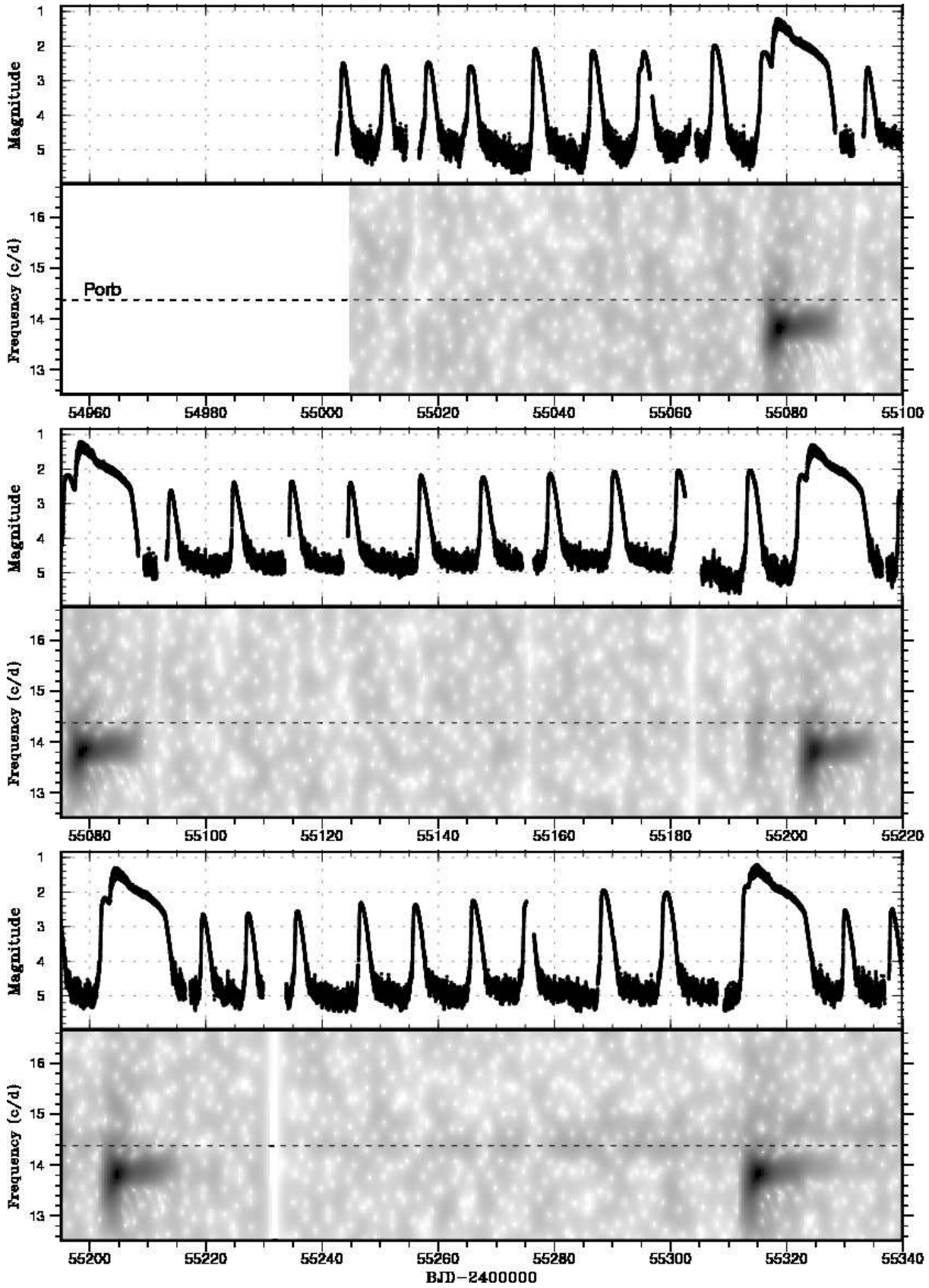


Fig. 3. The same as figure 2 but for six supercycles showing some of detailed features. The upper panel of each supercycle shows the light curve and the lower panel does the power spectrum around the orbital frequency region. The horizontal dash line represents the orbital frequency.

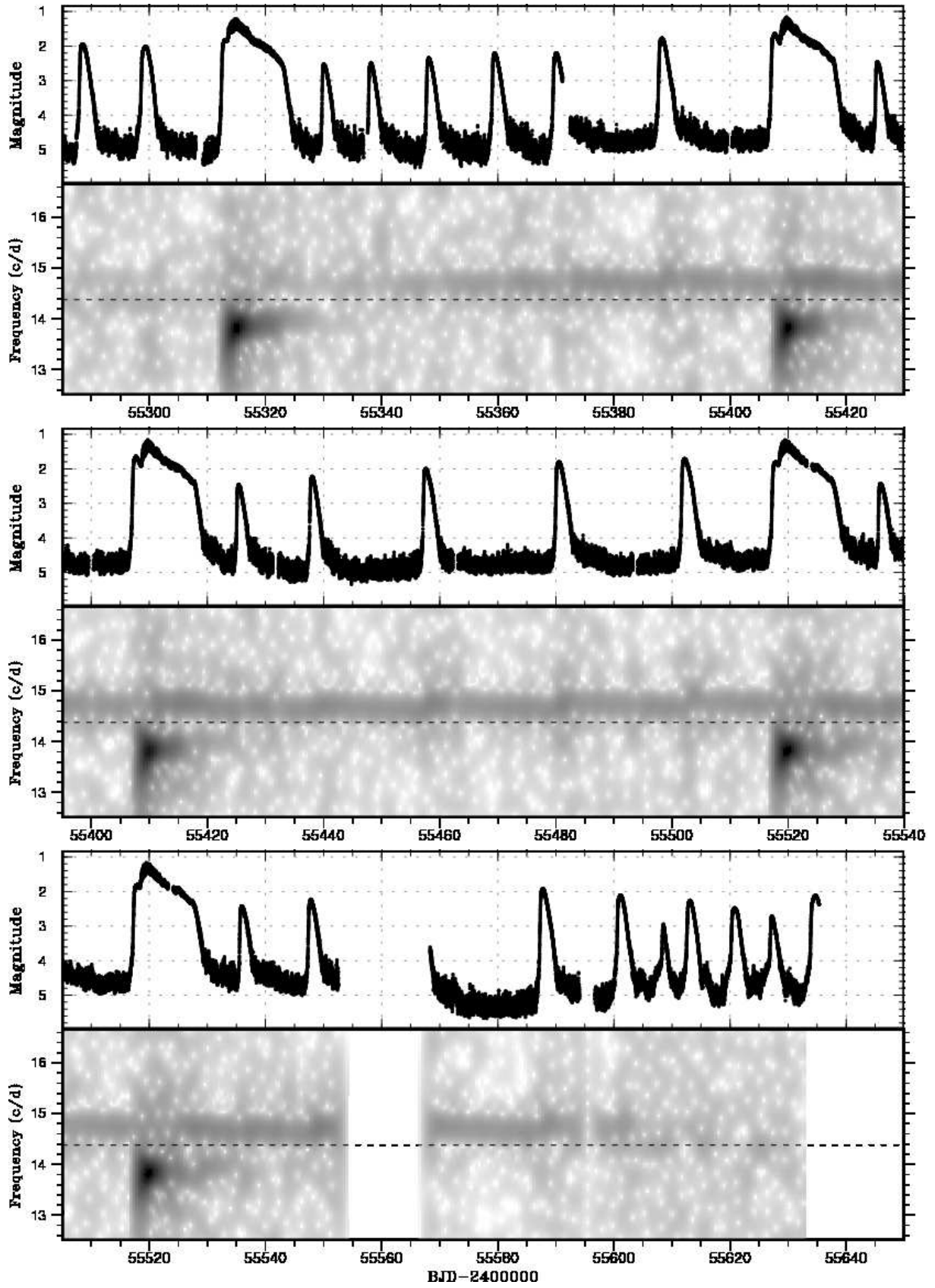


Fig. 3. (continued)

the dashed line. We can see that the strongest signal in the power spectrum occurs at a frequency of around 13.8 c/d, corresponding to that of ordinary (positive) superhumps whenever a superoutburst occurs – a well-known fact concerning SU UMa stars. Its higher harmonics are all visible in the middle panel of figure 2, indicating the nonsinusoidal waveform of the positive superhump light variation.

The most interesting aspect of the dynamic spectrum is the appearance of "negative hump" at frequency around 14.7 c/d. These are humps with a period shorter than the binary's orbital period (a few percent shorter than the orbital period). Although the origin of negative superhumps has not been yet firmly established, the standard interpretation is that of retrograde nodal precession of a tilted disk (e.g., Harvey et al. 1995, Montgomery, Martin 2010, Wood et al. 2011). Since there is no viable alternative model, we adopt the model of a tilted disk as a working hypothesis, and examine the Kepler data based on this model. In this picture the negative superhump is produced when the accretion disk is tilted from the binary's orbital plane, and its nodal line precesses retrograde, and the negative-superhump periodicity is produced by the synodic period between the retrograde precessing disk and the orbiting secondary star. The light variation with the negative-superhump period is thought to be produced by a periodic change in the dissipation of the kinetic energy of the gas stream from the secondary star with varying depth of potential well in the disk as it sweeps around the tilted disk (see Wood et al. 2011). When the accretion disk is coplanar with the orbital plane, the gas stream collides with the disk at the outer rim and this produces "orbital humps" with the binary's orbital period.

Negative superhumps for the Kepler data of V344 Lyr have been already discussed from the standpoint of a tilted disk by Wood et al. (2011). In V344 Lyr, negative superhumps appeared both in quiescence and in normal outbursts; on another occasion the signature of the negative superhump disappeared. A signature of the orbital hump appeared from time to time but these two signals did not seem to exist simultaneously. We can see in the lower panel of figure 2 that a signal of the negative superhump appeared in the middle of supercycle No. 3 in V1504 Cyg. It is not clear when this signal first appeared but a very weak signal is recognized at around BJD 2455250. Its intensity increased with time, and this signal became very clearly visible after BJD 2455350 in the later half of supercycle No. 4. It continued to be seen until BJD 2455600, and then tapered off.

Most interestingly, the appearance of negative superhumps is strongly correlated with the duration of the quiescence interval of outbursts; the quiescence interval between two outbursts becomes longer when the negative superhump appears. That is, the appearance of negative superhumps tends to reduce the frequency of normal outbursts. The same type of phenomena has already been observed in other SU UMa stars with high mass-transfer rates, such as V503 Cyg (Kato et al. 2002, Kato et al. 2013) and ER UMa (Ohshima et al. 2012). Cannizzo et al.

(2012) also noticed this in the Kepler light curve of V344 Lyr. In our Kepler data we basically confirm the findings of Kato et al. (2002), Kato et al. (2013), and Ohshima et al. (2012) that the existence of negative superhump suppresses frequent occurrence of normal outbursts.

A similar type of difference in supercycles has already been noticed in light curves of VW Hyi (a prototype SU UMa star). Smak (1985) has classified them into two types: Type L supercycle in which the interval of the last two normal outbursts is longer than 30 d and Type S in which it is shorter than 23 d, where the average supercycle length of VW Hyi is ~ 180 d. The number of normal outbursts in the Type L supercycle is small, while that in Type S is roughly twice as large as that of Type L. In Type L supercycle of VW Hyi, the quiescence interval between normal outbursts increases monotonously with the advance of the supercycle phase, while in Type S it increases till the intermediate phase of supercycle, but decreases in its latter half. Smak (1985) has found no correlation between these two supercycle types with either preceding or following superoutbursts, and with other supercycle properties. Thus, the origin of these two types remains to be a mystery.

Here, we make use of Smak's symbols of Type L and Type S supercycles in our case of V1504 Cyg. We define here that the Type L supercycle is that in which the quiescence interval between two normal outbursts is relatively "long", but the number of normal outbursts during a given supercycle is small, while the Type S is that in which the quiescence interval between two normal outbursts is "short", but the number of normal outbursts during a supercycle is large. However, we note that Smak's distinction for Types L and S in VW Hyi concerns only the last two normal cycles, while it applies to most of the normal outburst intervals in our case. In figure 2 we find that in V1504 Cyg, supercycles No. 4 and No. 5 correspond to Type L, while supercycle No. 2 corresponds to Type S.

Phenomenologically speaking, we may understand from the Kepler data that the Type L supercycle is accompanied by negative superhumps while the Type S supercycle does not have negative superhumps. Furthermore, if we adopt a tilted disk as the origin of the negative superhump, we can understand how the two distinct types of supercycle, Type L and Type S, are produced, as discussed below.

V1504 Cyg belongs to SU UMa stars with high mass-transfer rates since their supercycle lengths are short (i.e., its mean value of around 110 d), showing frequent normal outbursts. Most normal outbursts in V1504 Cyg are expected to be of outside-in type, which has been confirmed by the observed shape of the outburst light curve, i.e., a rapid rise to the outburst maximum and a slow decline from the maximum [see, Smak (1984); he calls such an outburst "type A outburst"]. Cannizzo et al. (2012) also mentioned the same view.

If the disk is co-planar with the binary orbital plane, the gas stream leaving the inner Lagrangian point of the secondary reaches the outer rim of the disk. On the other

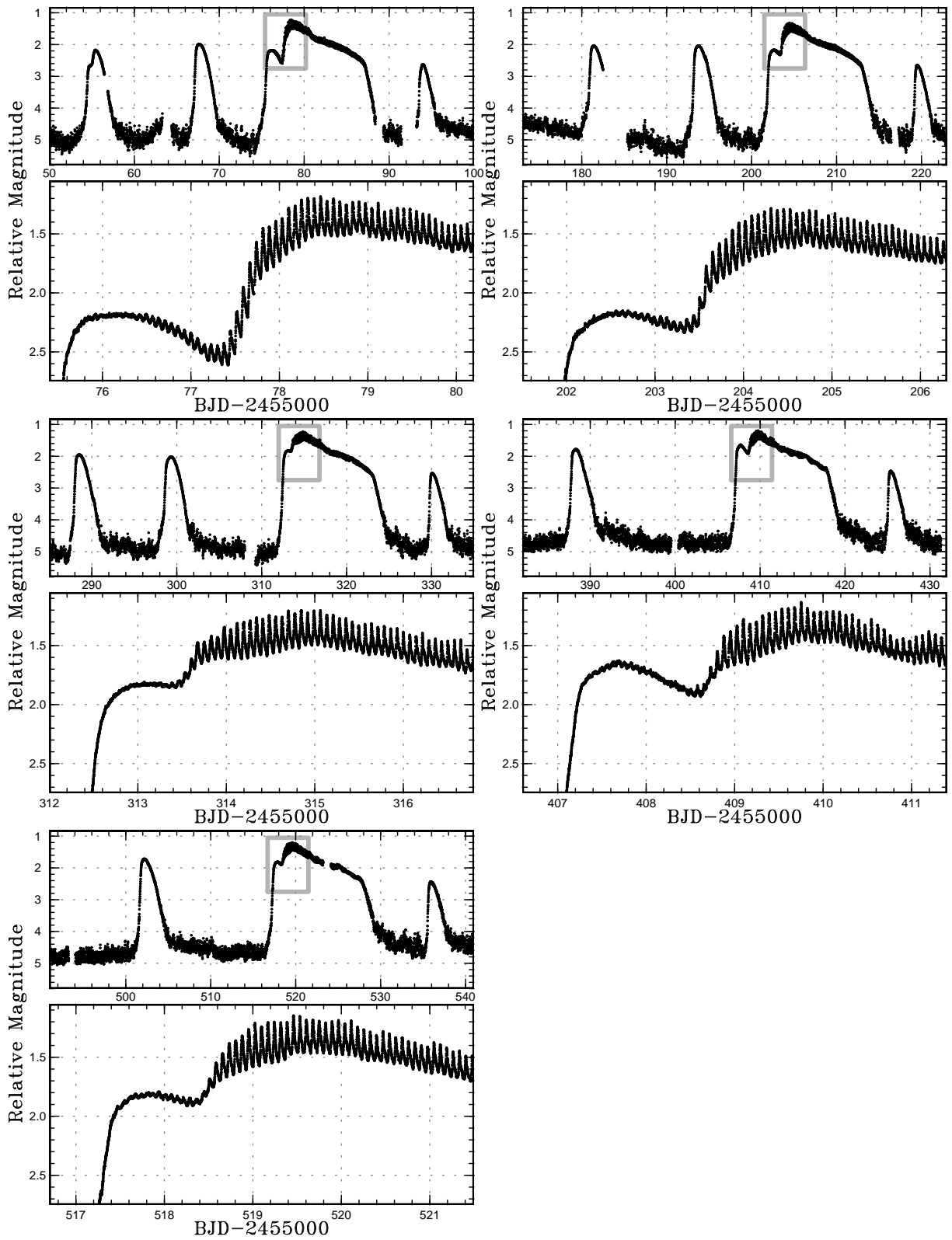


Fig. 4. Enlarged light curves of the five superoutbursts of V1504 Cyg around their start. The Kepler data were averaged to 0.01 d and 0.0005 d bins in the global and enlarged figures, respectively.

hand, if the disk is tilted, the gas stream sweeps over the tilted disk, but it hits the outer rim twice during the synodic period between the retrograde precessing tilted disk and the orbiting secondary star (i.e., the negative-superhump period) and at other times it reaches the inner part of the disk. In such a case matter reaching the outer edge is effectively reduced, even if the mass-transfer rate from the secondary remains constant. If all normal outbursts during a supercycle are of outside-in types, the normal outburst cycle is then lengthened accordingly, because the recurrence time of normal outburst is essentially determined by the mass-supply rate at the disk's outer edge in the case of an outside-in outburst. This explains why the number of normal outbursts during a given supercycle is small in the Type L supercycle. We note here that the above discussion is based on an assumption of outside-in type outburst. If mass is supplied to the inner part of the disk via a tilted disk, the probability of occurrence of inside-out outburst will increase. Therefore we must be careful to know whether an outburst is outside-in or inside-out.

Thus, it is now understood that whether the negative superhump exists or not makes a distinction between Type L and S supercycles in V1504 Cyg; that is, the former is accompanied by negative superhumps and the latter is without them. However, we should note that there are intermediate types of supercycles between these two extreme cases. For instance, in our supercycle No. 6, in which our Kepler data are incomplete, a signal of negative superhumps is visible in its early phase (during a period of ~ 70 d from BJD 2455530 to BJD 2455600) during which a frequent occurrence of normal outbursts is suppressed, but it recovered as the signal of negative superhumps tapered off around BJD 2455600.

Although we understand a general picture concerning negative superhumps and the occurrence of normal outbursts, a big problem remains to be solved: how on earth the negative superhump (i.e., a tilted disk) is produced and how it is maintained for a long time. We discuss the nature of negative superhumps in subsection 3.4 again.

3.2. *The Start of a Superoutburst*

Next, we examine how a superoutburst is initiated in V1504 Cyg. It has turned out that all superoutbursts observed in the Kepler data of V1504 Cyg are of precursor-main type. Figure 4 shows enlarged light curves of five superoutbursts of V1504 Cyg in our data and one of such light curves has already been shown in figure 75 of Kato et al. (2012); also see the Kepler light curves shown in Cannizzo et al. (2012). We can see very clearly in figure 4 that periodic humps (which have turned out to be “superhumps” based on their period; see the power spectrum in figure 3) appear around the maximum of the precursor (that is, a triggering normal outburst); they continue to grow in amplitude passing through the local light minimum to the main superoutburst phase, and the time of maximum amplitude of superhumps agrees fairly well with that of the light maximum of the superoutburst. This is exactly a picture envisioned in the original thermal-tidal

model (TTI model) proposed by Osaki (1989).

Although similar phenomena have been observed before in other stars, e.g., V436 Cen (Semiñuk 1980), and QZ Vir (T Leo) (Kato 1997), the Kepler light curve shown here in figure 4 is unprecedentedly clear in this respect. It is quite evident from figure 4 that superhumps are not a result of superoutburst but rather superhumps (therefore the tidal instability) are most likely the cause of the superoutburst since superhumps start to grow near the precursor maximum. The superhump and superoutburst are so much entwined that one is almost difficult to find any interpretation other than the TTI model, that is, the tidal instability triggers a superoutburst in V1504 Cyg.

Furthermore, Kato et al. (2012) have found transient low-amplitude superhumps in the descending branch of a normal outburst just prior to superoutburst No. 1 (see their figure 78). Similar superhump signatures are also seen in our power spectrum of figure 3 for normal outbursts just prior to superoutbursts No. 2 and No. 3. This phenomenon is very well understood as the failed superhump (or the aborted superhump) discussed by Osaki, Meyer (2003), (see their figure 4).

It is then natural to interpret the periodic humps in the case of VW Hyi discussed by Vogt (1983) as the same sort of phenomenon, (i.e., “failed superhumps”). We believe that the first question concerning about enhanced mass transfer prior of a superoutburst raised by Smak (1996) has been clarified by the Kepler light curve of V1504 Cyg.

As for the second problem raised by Smak (1996), V1504 Cyg shows the precursor-main type superoutburst and the superhump appears in the precursor stage and its amplitude grows with the start of the main superoutburst and it reaches maximum almost with the superoutburst light maximum, that is, the sequence of events observed in V1504 Cyg is exactly as predicted by the original TTI model.

We do not need to address to cases of other SU UMa stars in which no precursor is observed and in which superhumps appear in one or two days after superoutburst maximum. These superoutbursts are understood in the TTI model as follows: in such a superoutburst the disk expands to reach the tidal truncation radius, passing the 3:1 resonance radius during a triggering normal outburst and the viscous plateau stage begins first and then superhumps grow later, as discussed in Osaki, Meyer (2003) and in Osaki (2005) where such a superoutburst is called “Type B” superoutburst. These superoutbursts are expected to occur in low mass-transfer SU UMa systems, which are more numerous in number as compared with high mass-transfer systems such as V1504 Cyg and V344 Lyr.

Let us now turn our attention to the pure thermal instability model advocated by Cannizzo and his group. Cannizzo et al. (2010) made numerical simulations of light curves based on the pure thermal-viscous limit cycle instability and compared their results to the Kepler light curve of V344 Lyr. The Kepler light curves of V344 Lyr also show precursors in superoutbursts which these authors called “shoulders”. These authors succeeded in re-

producing shoulder-like structure in their superoutburst light curve but the duration of the shoulder in their simulations was found to be too long compared with those of V344 Lyr. Our criticism to their pure thermal instability model for their explanation of the precursor is not on this point but rather on the following point.

In Cannizzo et al. (2010) simulations, a precursor or “shoulder” is produced when the thermal instability starts in the inner part of the accretion disk and the heating front propagates outward but stagnates in the middle of disk for a little while. The heating front restarts to propagate outward to reach the outer edge of the disk which lies at the tidal truncation radius. The long superoutburst ensues. The shoulder is produced when the heating front stagnates in the middle of accretion disk in this model. However, the heating front which stagnates should be never reflected back as a cooling front to produce a superoutburst in their model. This is because the very outburst would have become merely a short normal outburst if it had been reflected. That is, in order to have a long superoutburst in their model, the heating front has to propagate all the way to the outer edge of disk, never being reflected.

Kepler light curves are optical light curves but it is known that the dip between the precursor and main becomes deeper in observations of shorter wavelength, e.g., in the Voyager far-ultraviolet observations of VW Hyi (Pringle et al. 1987), and in EUV observations of OY Car (Mauche, Raymond 2000). In shorter wavelength, the precursor looks like a separate normal outburst. That means that the heating front has to be reflected as a cooling front in the precursor. This observational evidence clearly contradicts with the pure thermal instability model advocated by Cannizzo and his group, because deep dips are never produced in their model.

On the other hand, in the TTI model the precursor is understood as a result of merging of triggering normal outburst with the main body of superoutburst. The degree of merging depends on individual stars and individual superoutbursts, sometimes a precursor is clearly separated from the main superoutburst and looks almost like a normal outburst, sometimes these two merge into one continuation. As discussed in Osaki (2005), in the case of TTI model the heating front is reflected at the outer edge as a cooling front in the triggering normal outburst in the “Type A” superoutburst in which the outer edge of the disk exceeds the 3:1 resonance radius but below the tidal truncation radius. The tidal instability (and thus superhumps) ensues in this triggering normal outburst. As superhumps grow in amplitude, the tidal dissipation is increased in the outer part of the disk and it eventually rekindles hot transition in the outer part of the eccentric disk, which affects most strongly to optical light. A new separate heating front propagates from outer part inward (i.e., a superoutburst is initiated) while the cooling front is still propagating inward. Depending on the relative position of these two fronts, the depths of the precursor dip differ. This explains why the depths of the dip differ in observations of different wavelength and in different stars

in TTI model.

As discussed by Schreiber et al. (2004), in order to explain the precursor observed in SU UMa stars, the cooling front has to propagate inward. Cannizzo et al. (2010) model cannot satisfy this requirement and thus the pure thermal instability model is not a viable model for precursor-main type superoutburst in this respect.

3.3. Negative Superhump and Disk Radius Variation

As can be seen in the power spectrum of figure 3, the negative superhump exists almost always during two supercycles No. 4 and No. 5, and some systematic variation in frequency is barely visible in these figures. We thus made a detailed analysis of the frequency variation of the negative superhump using the Kepler data during the period from day 380 to day 550 covering a complete supercycle, No. 5. Figure 5 illustrates the results for the frequency variation of the negative superhump together with the light curve of V1504 Cyg. We calculated its frequency using a data window of 4 d with a time step of 0.5 d. We used phase-dispersion minimization (PDM: Stellingwerf 1978) for obtaining the period, and used Fernie (1989) and Kato et al. (2010) for estimating 1- σ errors in the period. During the superoutburst plateau, we first subtracted the signal of positive superhumps and applied the analysis to the residual signal. Since the amplitude of the negative superhumps was smaller than that of positive superhumps, particularly at around the peaks of the superoutbursts, there were relatively large errors in estimating the period of negative superhumps during a superoutburst.

In figure 5 we find a characteristic variation in the negative-superhump frequency during a supercycle, such as is reminiscent of the disk-radius variation in a supercycle of the TTI model shown in figure 1. In fact, if we accept a tilted disk model for the negative superhump, its frequency has turned out to be a good measure of the disk radius. If we use a simplified model for retrograde precession of a tilted disk, the frequency of the negative superhump is given by (see, Larwood 1998)

$$\nu_{\text{NSH}} = \nu_{\text{orb}} \left\{ 1 + \left(\frac{3}{7} \frac{q}{\sqrt{1+q}} \cos\theta \right) \left(\frac{R_d}{A} \right)^{3/2} \right\}, \quad (1)$$

where ν_{NSH} and ν_{orb} are the frequency for the negative superhump and binary orbital frequency, respectively, $q = M_2/M_1$ is the mass ratio of the binary, R_d the disk radius, A is the binary separation, θ is the tilt angle of the disk to the binary orbital plane. We assume $\cos\theta \simeq 1$ for a slightly tilted disk. Furthermore if we assume the mass ratio $q = 0.2$ for V1504 Cyg, we can estimate the disk radii, $R_d/A \simeq 0.34, 0.43,$ and 0.52 for $\nu_{\text{NSH}} = 14.6, 14.7$ and 14.8 c/d, respectively from equation (1).

We can see in figure 5 that the disk radius, R_d , shows a saw-tooth pattern with an expansion of the disk in each normal outburst accompanied by contraction during quiescence; also the average radius of the saw-tooth pattern increases with the advance of supercycle phase. Finally, the last normal outburst (which corresponds to a triggering outburst, i.e., a precursor stage of superoutburst) brings the disk to a critical radius, (i.e., the tidal 3:1 reso-

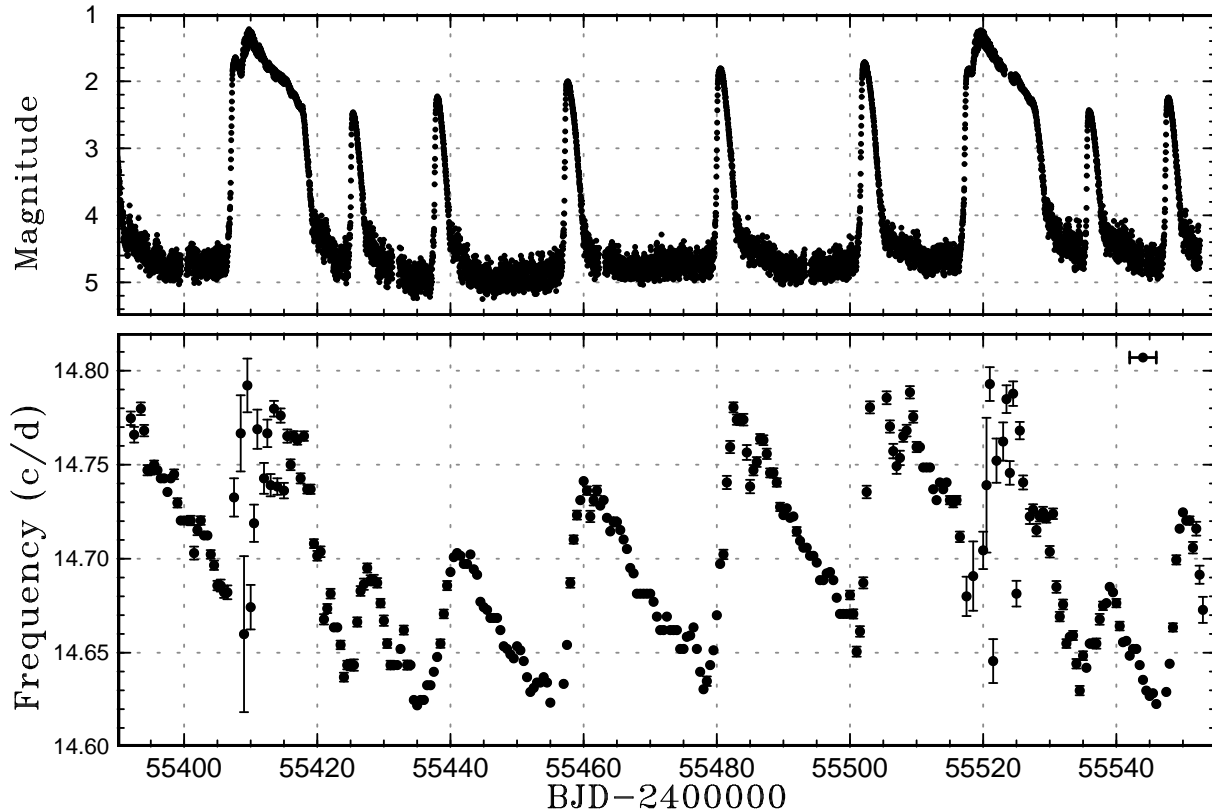


Fig. 5. Time evolution of frequency of the negative superhump covering a complete supercycle No. 5 from BJD 2455390 to 2455550. The upper panel shows light curve while the lower panel does variation in negative superhump frequency in units of cycle per day. The frequency (or period) was calculated by using the PDM method with a window width of 4 d and a time step of 0.5 d. The window width is indicated as a horizontal bar at the upper right corner of the lower panel. The Kepler data were averaged to 0.0005 d bins and the error bars in the lower panel represent $1\text{-}\sigma$ errors in the periods.

nance instability radius $R_{3:1}/A \sim 0.47$). A superoutburst ensues and a large amount of mass is drained from the disk during a superoutburst and, after the end of the superoutburst, the disk radius returns to a small value of radius, a picture exactly predicted by the TTI model as shown in figure 1. Figure 5 exhibits clearly how the angular momentum is accumulated in the disk during a supercycle. The most important prediction of the TTI model concerns the disk-radius variation during a supercycle, but its observational test was difficult until Kepler observations. The Kepler data of V1504 Cyg with the negative superhump now opens a new way to the test of this prediction.

3.4. Coexistence of Positive and Negative Superhumps

As seen in the two-dimensional power spectra of figure 2 and figure 3, the positive and negative superhumps can co-exist during a superoutburst, such as the superoutburst No. 4 and No. 5. Figure 6 illustrates a light curve of the superoutburst No. 4 which clearly shows a beating phenomenon of the positive and negative superhumps. The lowest panel of figure 6 shows a PDM diagram in this superoutburst in which two signals at periods 0.067764(10) d (the negative superhump) and 0.072183(4) d (the positive superhump) are visible. The beat period of these two waves is estimated to be about 1.1 d and the amplitude

variations with this beat period are seen in the middle panel of figure 6.

This means that the disk in V1504 Cyg develops tilted and eccentric form simultaneously. Figure 7 shows phase-averaged light curves of the positive superhumps (upper panel) and of the negative superhumps (lower panel) for this superoutburst.

The light curve of the positive superhump shown in figure 7 is a typical one for the ordinary superhump seen during a superoutburst, that is, a rapid rise to maximum and slow decline sometimes accompanied with a secondary maximum. On the other hand, the light curve of the negative superhump shows more or less a sinusoidal waveform. For comparison, we show a phase-averaged light curve of the negative superhump in quiescence with a period 0.068076 d during 8 d of BJD 2455440–448 in figure 8. Wood et al. (2011) discussed the Kepler light curve of the negative superhump in quiescence for V344 Lyr, showing that it is approximately saw-toothed with a rise time roughly twice the fall time. Figure 8 shows the same wave pattern as that of V344 Lyr. As discussed by Wood et al. (2011) and mentioned already in subsection 3.1, the quiescence light curve of the negative superhump is understood in terms of gas stream hitting the different part of the disk. We discuss on a possible origin of sinusoidal

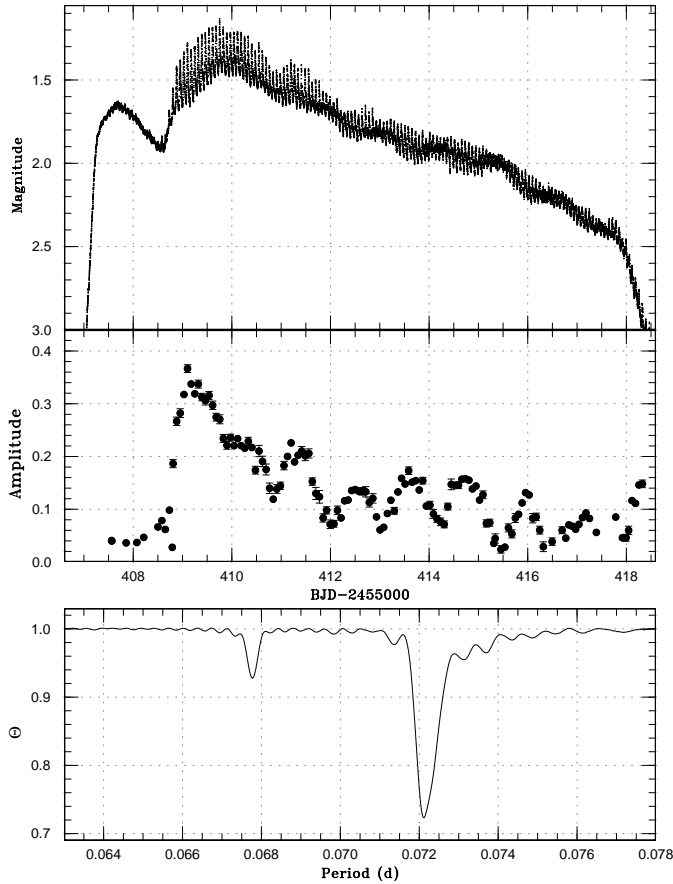


Fig. 6. (Upper:) A light curve of the superoutburst No. 4 showing beating phenomenon between the positive superhump wave and the negative superhump one. The Kepler data were averaged to 0.0005 d bins. (Middle:) Amplitudes of positive superhumps. The amplitudes were determined with the method in Kato et al. (2009). (Lower:) PDM analysis. Both positive and negative superhumps were present.

waveform of the negative superhump during the superoutburst in Appendix.

Amplitudes (in flux) of negative superhumps in the superoutburst No. 4 and in neighboring quiescence are not so much different as seen from figures 2 and 3. In fact, the full amplitudes are 0.04 mag and 0.35 mag, respectively, as seen in figure 7 and figure 8. Since the magnitude difference between the superoutburst and quiescence is about 3 mag in V1504 Cyg, they are similar in flux units. This suggests that mass-transfer rate is not particularly enhanced during the superoutburst. This supports the TTI model rather than the EMT model.

4. Summary

(1) The long outburst of almost all of dwarf novae below the period gap is accompanied by superhumps. No dwarf novae showing a superoutburst and a well-defined supercycle and without superhumps, have yet been discovered. Since the superoutburst and superhumps are very much

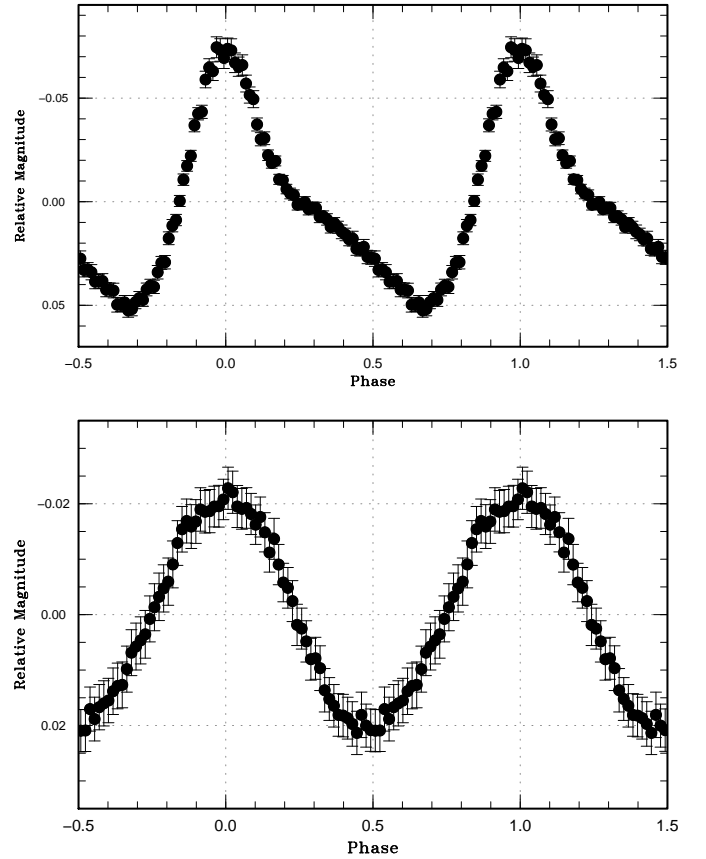


Fig. 7. Phase-averaged light curves of the positive superhump (upper), and of the negative superhump (lower) for the superoutburst No. 4. The periods used for the folding are 0.072183 d and 0.067764 d, respectively.

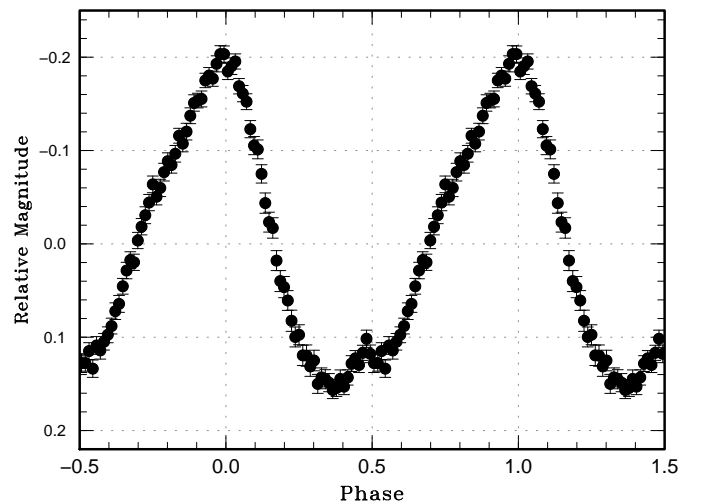


Fig. 8. Phase-averaged light curve of the negative superhump with a period 0.068076 d during quiescence for 8 d of BJD 245440-448 in V1504 Cyg.

entwined as demonstrated in figure 4, no models without taking into account the tidal instability properly seem to be correct and we believe that the TTI model is only a viable model for the superoutburst and superhumps of SU UMa stars.

(2) The periodic hump observed in the decline phase of a normal outburst just prior to the next superoutburst is found to be of superhump property and the orbital hump is not particularly enhanced in this phase in V1504 Cyg. We conclude that no enhancement of mass transfer from the secondary star exists in this phase and at the start of the superoutburst.

(3) The quiescence intervals between normal outbursts strongly depend on whether negative superhumps exist or not. We confirm that the conclusion of Ohshima et al. (2012) for ER UMa that the existence of negative superhumps tends to suppress the frequent occurrence of normal outbursts. Two types of supercycles are recognized in V1504 Cyg which are very similar to the Type L and Type S supercycles introduced by Smak (1985) in the case of VW Hyi. The Type L supercycle is a supercycle in which the number of normal outbursts is small, typically 5 to 6, while in the Type S supercycle it is twice as large (typically around 10) as that of Type L in V1504 Cyg. The Type L supercycle is accompanied by the negative superhump, while Type S is without the negative superhump.

(4) Most of normal outbursts observed in V1504 Cyg are of the outside-in type. If so, lengthening the quiescence intervals when the negative superhump appears is understood as to be due to a decrease in mass supply *at the outer edge*, of the tilted disk as gas stream flows over the edge and reaches its inner part in such a case.

(5) The frequency of the negative superhump varies systematically during a supercycle. If we adopt a tilted-disk model for the origin of the negative superhump, its frequency represents retrograde precession rate of the tilted disk. Using this variation as an indicator of the disk-radius variation, we found that the observed disk-radius variation in V1504 Cyg fits very well with a prediction of the TTI model.

(6) The positive and negative superhumps can coexist, seen as a beat phenomenon of these two waves in the light curve of superoutburst No. 4 in V1504 Cyg. This means that the disk can take eccentric and tilted form simultaneously. The amplitude of the negative superhump during the superoutburst is not particularly enhanced in flux units as compared with that of neighboring quiescence. This suggests no enhancement of mass-transfer rate during the superoutburst, which supports the TTI model rather than the EMT model for the origin of the superoutburst.

(7) We summarize major consequences of the three models discussed in this paper in the lower part of table 1.

We are grateful to Dr. Makoto Uemura for his help in retrieving the Kepler data. One of authors (Y. Osaki) thanks the organizers of a conference held in Warsaw, 2012 September “Accretion Flow Instabilities: – 30 years of

thermal-viscous instability” for encouraging him to participate, of which experience stimulated him to come back to research in astronomy after a 7 yr absence. He also would like to express his sincere thanks to Dr. Friedrich Meyer at Max-Planck-Institut für Astrophysik for encouraging him to write this paper and Professor Hiromoto Shibahashi for enlightening discussions about power spectra. This work was partly supported (TK) by the Grant-in-Aid for the Global COE Program “The Next Generation of Physics, Spun from Universality and Emergence” from the Ministry of Education, Culture, Sports, Science and Technology (MEXT) of Japan. We thank the Kepler Mission team and the data calibration engineers for making Kepler data available to the public.

Note added in proof (April 30, 2013): We have replaced our figure 5 of the original version to a new one because we made a mistake of 2 d in time axis of our lower panel of figure 5 in the first version of a preprint, which was submitted to astro-ph on December 7, 2012, (arXiv:1212.1516v1), and the mistake was corrected in version 2 submitted on January 6, 2013 (arXiv:1212.1516v2). Figure 5 is now the corrected one. This mistake crept in, when we inadvertently used time of local frequency at that of the starting date of the window instead of the correct one (i.e., the middle of the window). We thank Dr. Smak who first noticed this error (Acta Astron, 63, 109, 2013). We notified him about our mistake on this point by e-mail on January 7, 2013.

Appendix 1. Waveform of negative superhump during a superoutburst

The different form of the light curve of the negative superhump during a superoutburst from that of quiescence may suggest that the origin of its light variation is different between superoutburst and quiescence. Let us now discuss the origin of light variation of the negative superhump during a superoutburst. During superoutbursts the disk component will play an important role besides that of gas stream in light variation of negative superhump. Then a question arises why its waveform is sinusoidal if the disk component contributes.

Here we propose a following explanation. Let us consider an eigenmode of oscillation of an accretion disk in which the unperturbed state is co-planar with the binary orbital plane. Here we use the cylindrical coordinates with (r, φ, z, t) in the inertial frame of reference where the center of the coordinates is chosen to be the center of the disk, i.e., the central white dwarf, the azimuthal angle φ is measured in the direction of the binary orbital motion, and the z -axis is that of the binary orbital plane. An eigenmode displacement vector is then written as

$$\xi(r, \varphi, z, t) = (\xi_h, \xi_z) \cos(m\varphi - \omega t), \quad (\text{A1})$$

where ξ is a displacement vector, ω is an eigenfrequency, m is azimuthal wave number, and ξ_h, ξ_z are horizontal and vertical displacements and this mode is denoted as a mode (m, ω) with azimuthal wave number m and eigenfrequency

ω .

We do not discuss on the excitation mechanism of tilted disk but we assume here that the disk is tilted with a finite tilt angle θ where $\theta \ll 1$, for simplicity. A tilt of disk is understood to be one of eigenmodes with $m = 1$ and $|\xi_h| \ll |\xi_z|$, $\xi_z \simeq \theta r$ and an eigenfrequency given by angular frequency of retrograde precession $\omega = \Omega_{\text{pr}} < 0$. This mode itself does not produce any light variation. In order to understand light variation of tilted disk, we need to consider an interaction of this mode with the tidal field of the secondary star. The tidal perturbing potential in the accretion disk by the secondary star is expressed by

$$\phi(r, \varphi, z, t) = \phi_m(r, z) \cos(m(\varphi - \Omega_{\text{orb}}t)), \quad (\text{A2})$$

where Ω_{orb} is the angular frequency of the binary orbital motion and $m = 1, 2, 3, \dots$ is azimuthal wave number. The tidal perturbation potential produces deformation in the accretion disk which is described by (see, Lubow 1991, Lubow 1992, Kato 2012)

$$\xi_{\text{D}}(r, \varphi, z, t) = \xi_{\text{D},m}(r, z) \cos(m(\varphi - \Omega_{\text{orb}}t)), \quad (\text{A3})$$

where suffix D denotes deformation.

The wave-wave interaction of the tilt mode with the tidal deformation mode produces $(m - 1, m\Omega_{\text{orb}} - \Omega_{\text{pr}})$ mode. In this interaction, the most important one is that of $m = 1$, that is, a mode with $(0, \Omega_{\text{orb}} - \Omega_{\text{pr}})$. This mode is independent of the azimuthal angle φ and the time dependence of $\sin\{(\Omega_{\text{orb}} - \Omega_{\text{pr}})t + \delta_0\}$, where δ_0 is a constant phase. That is, this mode produces a sinusoidal time variation with the negative superhump period $P_{\text{NSH}} = 2\pi/(\Omega_{\text{orb}} - \Omega_{\text{pr}})$ where $\Omega_{\text{pr}} < 0$ is retrograde nodal precession rate of a tilted disk. This can produce light variation even with the pole-on geometry, i.e., in the case of inclination angle $i = 0$. Light variation with the negative superhump period observed during a superoutburst in V1504 Cyg can be explained by this disk component produced by wave-wave interaction between a tilt mode and the tidal deformation with $m = 1$ besides the gas stream component.

References

- Buat-Ménard, V., & Hameury, J.-M. 2002, *A&A*, 386, 891
 Cannizzo, J. K. 1993, in *Accretion Disks In Compact Stellar Systems*, ed. C. Wheeler (Singapore: World Scientific), p. 6
 Cannizzo, J. K., Smale, A. P., Wood, M. A., Still, M. D., & Howell, S. B. 2012, *ApJ*, 747, 117
 Cannizzo, J. K., Still, M. D., Howell, S. B., Wood, M. A., & Smale, A. P. 2010, *ApJ*, 725, 1393
 Cleveland, W. S. 1979, *J. Amer. Statist. Assoc.*, 74, 829
 Fernie, J. D. 1989, *PASP*, 101, 225
 Harvey, D., Skillman, D. R., Patterson, J., & Ringwald, F. A. 1995, *PASP*, 107, 551
 Hellier, C. 2001a, *Cataclysmic Variable Stars: how and why they vary* (Berlin: Springer-Verlag)
 Hellier, C. 2001b, *PASP*, 113, 469
 Hirose, M., & Osaki, Y. 1990, *PASJ*, 42, 135
 Ichikawa, S., Hirose, M., & Osaki, Y. 1993, *PASJ*, 45, 243
 Kato, S. 2012, *PASJ*, submitted
 Kato, T. 1997, *PASJ*, 49, 583
 Kato, T., et al. 2013, *PASJ*, 65, 23
 Kato, T., et al. 2009, *PASJ*, 61, S395
 Kato, T., Ishioka, R., & Uemura, M. 2002, *PASJ*, 54, 1029
 Kato, T., et al. 2012, *PASJ*, 64, 21
 Kato, T., et al. 2010, *PASJ*, 62, 1525
 Koch, D. G., et al. 2010, *ApJL*, 713, L79
 Larwood, J. 1998, *MNRAS*, 299, L32
 Lasota, J.-P. 2001, *New Astron. Rev.*, 45, 449
 Lubow, S. H. 1991, *ApJ*, 381, 259
 Lubow, S. H. 1992, *ApJ*, 401, 317
 Mauche, C. W., & Raymond, J. C. 2000, *ApJ*, 541, 924
 Montgomery, M. M., & Martin, E. L. 2010, *ApJ*, 722, 989
 Murray, J. R. 1998, *MNRAS*, 297, 323
 Ohshima, T., et al. 2012, *PASJ*, 64, L3
 Osaki, Y. 1985, *A&A*, 144, 369
 Osaki, Y. 1989, *PASJ*, 41, 1005
 Osaki, Y. 1996, *PASP*, 108, 39
 Osaki, Y. 2005, *Proceeding of the Japan Academy, Series B*, 81, 291
 Osaki, Y., & Meyer, F. 2003, *A&A*, 401, 325
 Pringle, J. E., et al. 1987, *MNRAS*, 225, 73
 Schreiber, M. R., Hameury, J.-M., & Lasota, J.-P. 2004, *A&A*, 427, 621
 Semeniuk, I. 1980, *A&AS*, 39, 29
 Smak, J. 1984, *Acta Astron.*, 34, 161
 Smak, J. 1985, *Acta Astron.*, 35, 357
 Smak, J. 1996, in *IAU Colloq. 158, Cataclysmic Variables and Related Objects*, ed. A. Evans, & J. H. Wood (Dordrecht: Kluwer Academic Publishers), p. 45
 Smak, J. 2000, *New Astron. Rev.*, 44, 171
 Smak, J. 2004, *Acta Astron.*, 54, 221
 Smak, J. 2008, *Acta Astron.*, 58, 55
 Smak, J. 2009, *Acta Astron.*, 59, 121
 Smak, J. I. 1991, *Acta Astron.*, 41, 269
 Smith, A. J., Haswell, C. A., Murray, J. R., Truss, M. R., & Foulkes, S. B. 2007, *MNRAS*, 378, 785
 Stellingwerf, R. F. 1978, *ApJ*, 224, 953
 Still, M., Howell, S. B., Wood, M. A., Cannizzo, J. K., & Smale, A. P. 2010, *ApJL*, 717, L113
 Truss, M. R., Murray, J. R., & Wynn, G. A. 2001, *MNRAS*, 324, 1P
 van Paradijs, J. 1983, *A&A*, 125, L16
 Vogt, N. 1983, *A&A*, 118, 95
 Warner, B. 1995, *Cataclysmic Variable Stars* (Cambridge: Cambridge University Press)
 Whitehurst, R. 1988, *MNRAS*, 232, 35
 Wood, M. A., Still, M. D., Howell, S. B., Cannizzo, J. K., & Smale, A. P. 2011, *ApJ*, 741, 105